論文　**Original Paper**

Estimating the degree of mudstone compactional thinning: Empirical relationship between mudstone compaction and geochemical composition

Kentaro Izumi*[1, 2, 3], Ryota Suzuki*[4], Mutsuko Inui*[2]

Abstract: The empirical relationship between the degree of compactional thinning and geochemical composition for fully consolidated mudstones was proposed for the first time. New data were provided by sedimentological, ichnological, and geochemical analyses of the mudstone samples from the Eocene Naharigawa Formation, Kochi Prefecture, Japan. Based on these analyses, the degree of compaction of the Naharigawa mudstones as a percentage of shortening (C_{ms}) was calculated as 83.01 %. To quantitatively estimate the empirical relationship, the C_{ms} values for various mudstones, whose geochemical compositions are available by previous studies, were further calculated and compiled. As a result of the compilation, a significant and strong negative correlation between the C_{ms} values and CaO abundances ($r = -0.75$; $p < 0.05$) was recognized. Furthermore, the C_{ms} values show negative correlation between Ca concentrations normalized to terrigenous material (CaO/Al_2O_3, CaO/TiO_2) that are considered as proxies for relative contribution of non-terrigenous (i.e. biogenic) carbonates, although the recognized correlations are not statistically significant. These lines of evidence strongly suggest that the degree of physical compaction of muddy sediments is affected by carbonate contents. Although the obtained relationship may hold only for fully consolidated mudstones of the Paleogene or older ages, it is very helpful for quantitatively estimating the degree of compactional thinning for any mudstone-dominated succession, as long as the major element composition of the mudstone is determined.

Key words: mudstone, compaction, diagenesis, sedimentology, geochemistry, ichnology

1. Introduction

Sediment compaction is an important phenomenon in sedimentary basins, and causes distinct changes in the physical properties of sediments during burial (Velde, 1996; Lobza and Schieber, 1999; Schieber, 2003; Kochman and Matyszkiewicz, 2013). In general, sediment compaction leads to higher density (i.e. lower porosity) with depth via both mechanical and chemical processes. Mechanical compaction of fine-grained sediments differs from that of sands and carbonates (e.g. Devaney et al., 1986). Clays and muds have higher initial porosity (ca. 80 %) relative to coarser facies, and therefore are affected more by the mechanical compaction than other sediments (e.g. Inami and Hoshino, 1974; Velde, 1996). This leads to marked changes in the physical properties of mudstones with increasing burial depth. Mechanical compaction is a function of effective stress and dominates during early diagenesis, i.e. in the shallow parts of the basin down to 2 to 4 km depth (ca. 80 to 100 degrees C). Chemical compaction (e.g. dissolution and precipitation of minerals) dominates in deeper parts of the basin at higher stresses and temperatures.

Understanding the physical properties of fine-grained sediments with progressive burial is important for petroleum exploration, drilling and production, and a number of field and laboratory-based studies describing mudstone compaction have been published (e.g. Velde, 1996; Mondol et al., 2007). From these previous works, a variety of empirical relationships has been proposed to express the behavior of decreasing porosity as a function of increasing stress and/or burial depth (e.g. Mondol et al., 2007 and references therein).

Despite the rich array of data and consequent discussions on the porosity of muddy sediments, relatively few studies have focused on investigation and estimation of the degree of physical mudstone thinning resulting from compaction (Devaney et al., 1986; Lobza and Schieber, 1999; Kochman and Matyszkiewicz, 2013). It is generally considered that

*[1]国立環境研究所 生物・生態系環境研究センター
*[2]国士舘大学 理工学部
*[3]現所属：千葉大学教育学部
*[4]海老名市立有馬中学校

mechanical compaction is the most significant process for mudstone-dominated sequences, resulting in 50 % to up to 70 % compactional thinning (e.g. Devaney et al., 1986; Lobza and Schieber, 1999; Kochman and Matyszkiewicz, 2013), though more precise data about mudstone compactional thinning is required for a full understanding of the underlying processes. Assessing accurately the thickness changes of mudstones during compaction is important for estimating precise sedimentation rates, reconstructing and understanding cross stratification features, and interpreting specific sedimentary structures. Moreover, climatic signals potentially resolvable from mudstone successions can be compromised by the processes of compaction.

Kochman and Matyszkiewicz (2013) carried out experimental study for estimating the degree of compactional thinning of the Oxfordian bedded sediments, which are composed of marls, oolitic limestones, detrital limestones, and microbial biostromes of massive facies. As a result, their experiment showed that the amount of mechanical compaction differs depending on the facies. Namely, the amount of mechanical compaction is higher for marls and detrital sediments, whereas the biostromes that grew on the slopes of the carbonate buildups revealed only a small susceptibility to mechanical compaction due to the formation of a rigid framework and intensive early diagenetic cementation (Kochman and Matyszkiewicz, 2013).

According to Kochman and Matyszkiewicz (2013), it is presumed that the degree of mudstone compactional thinning decreases with increasing carbonate (~ biogenic and/or authigenic calcite/dolomite) content, though their specific relationship has not been proposed so far. Therefore, to address this issue, this study provides new data and compiles available data for the degrees of mudstone compactional thinning and carbonate proxies determined by geochemical data. We then propose the empirical relationship between the degrees of mudstone compaction and such carbonate proxies.

2. Methods for estimating the degree of mudstone mechanical compaction

Quantification of thinning by mudstone mechanical compaction is provided by various methods. Among them, the best and simplest way is to focus on differential compaction (Devaney et al., 1986). Initially hard material or early diagenetic concretions or nodules are very useful for quantifying mudstone compactional thinning (Potter et al., 2005). For examples, early diagenetic concretions or rapidly mineralized coprolites (i.e. Nakajima and Izumi, 2014) are the best materials. In these cases, when the thicknesses of mudstone laminae just above and adjacent to concretion/coprolite are h_{ini} and h_{fin}, respectively, compaction as a percentage of shortening (C_{ms}) can be described via $C_{ms} = (1 - h_{fin}/h_{ini}) * 100$ (Devaney et al., 1986; Kochman and Matyszkiewicz, 2013; **Fig. 1A**).

Another way for reconstructing the degree of mudstone compaction is to focus on invertebrate burrows. In particular, burrow aspect ratio (i.e. burrow width/burrow height) can also be used for assessing the mudstone compactional thinning (**Fig. 1B**), because most burrows are initially circular in cross-section (e.g. Devaney et al., 1986; Lobza and Schieber, 1999). In addition, sand-filled burrows within mudstones can also be used effectively for this purpose, by combining **Fig. 1A** and **Fig. 1B** approaches (**Fig. 1C**).

Although it is commonly believed that modern worm burrows have circular cross sections (i.e. initial burrow aspect ratio = 1, Lobza and Schieber, 1999), this hypothesis has not been hitherto verified by actual measurements. Therefore, this study actually analyzed aspect ratios of modern *Planolites*, a worm burrow commonly recognized in marine muddy sediments (e.g. Gerard and Bromley, 2008; Nishida et al., 2016), by using several published photographs.

3. Materials and analysis of this study

In this study, new data is provided based on the trace-fossil analysis and geochemical measurement of the Eocene Naharigawa Formation, Kochi Prefecture, southwest Japan.

Well-preserved trace-fossil assemblages are yielded in the clastic-rock successions of the Naharigawa Formation of the Muroto-Hanto Group, a Paleogene accretionary complex, which was originally deposited in an oceanic trough (e.g. Katto and Taira, 1978; Taira et al., 1980, 1988, 1992; Nara and Ikari, 2011; **Fig. 2A**). The Naharigawa Formation consists mainly of alternating beds of very coarse- to medium-grained, thick sandstone and mudstone, and thinly alternating beds of fine-grained sandstone and mudstone (Nara and Ikari, 2015). The formation is interpreted to have been deposited in a deep-sea channel-levee systems (Nara and Ikari, 2011). Previous studies reported the occurrence of a rich variety of trace fossils, including *Glockerichnus glockeri*?, *Helminthoraphe flexuosa*, *Lophoctenium*? isp., *Ophiomorpha* isp., *Paleodictyon minimum*, *Protovirgularia* isp., *Tasselia ordamensis* (Nara and Ikari, 2011, 2015). During our fieldwork, *Planolites* isp. and *Phycosiphon incertum* were newly discovered, and the former is the target trace fossil of this study.

Planolites isp. from the Naharigawa Formation is an

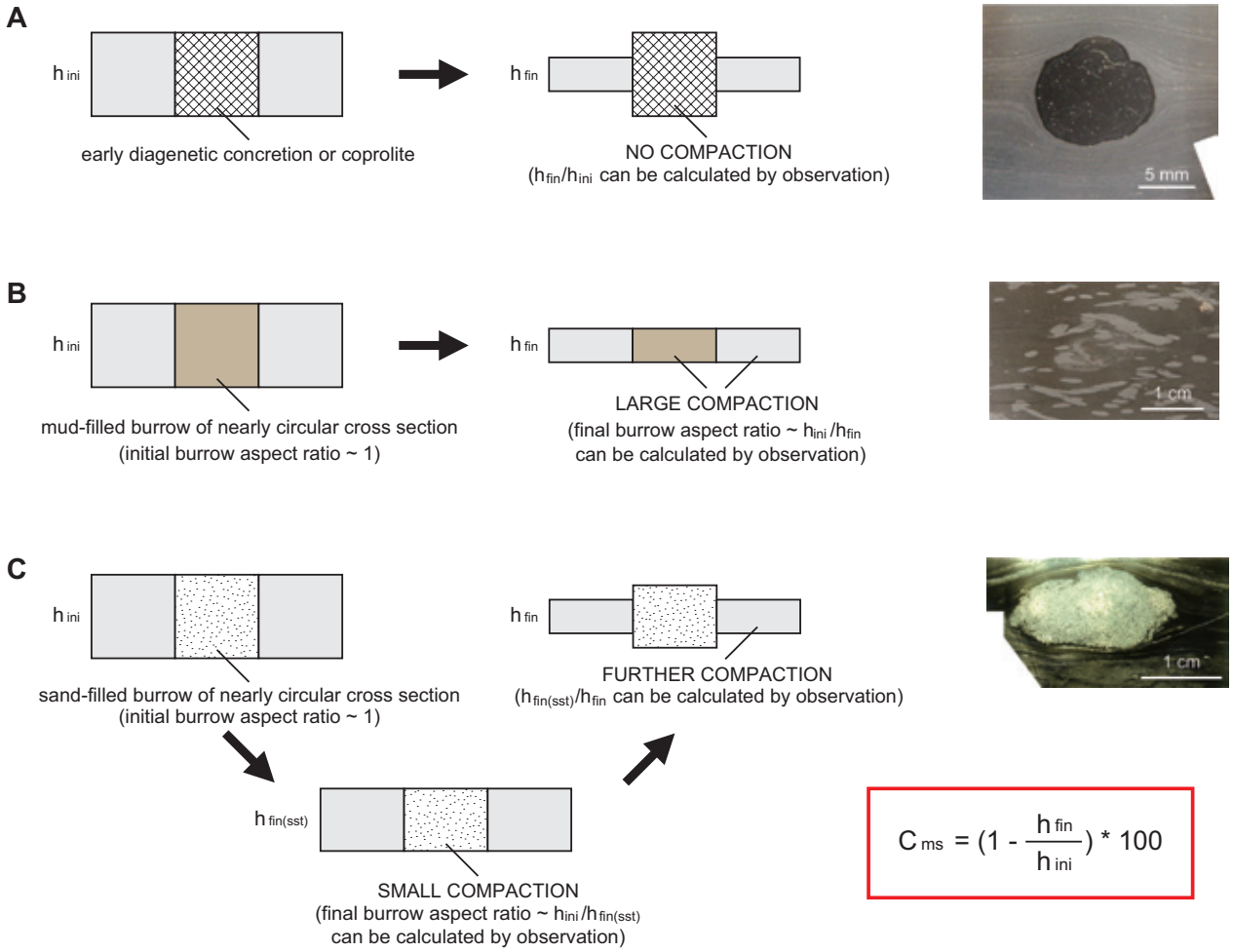

Fig. 1 Schematic illustration showing three methods (A, B, and C) for calculating the degree of mudstone compactional thinning. For detailed explanation of each method, see main text. Photograph in A is referred from Nakajima and Izumi (2014).

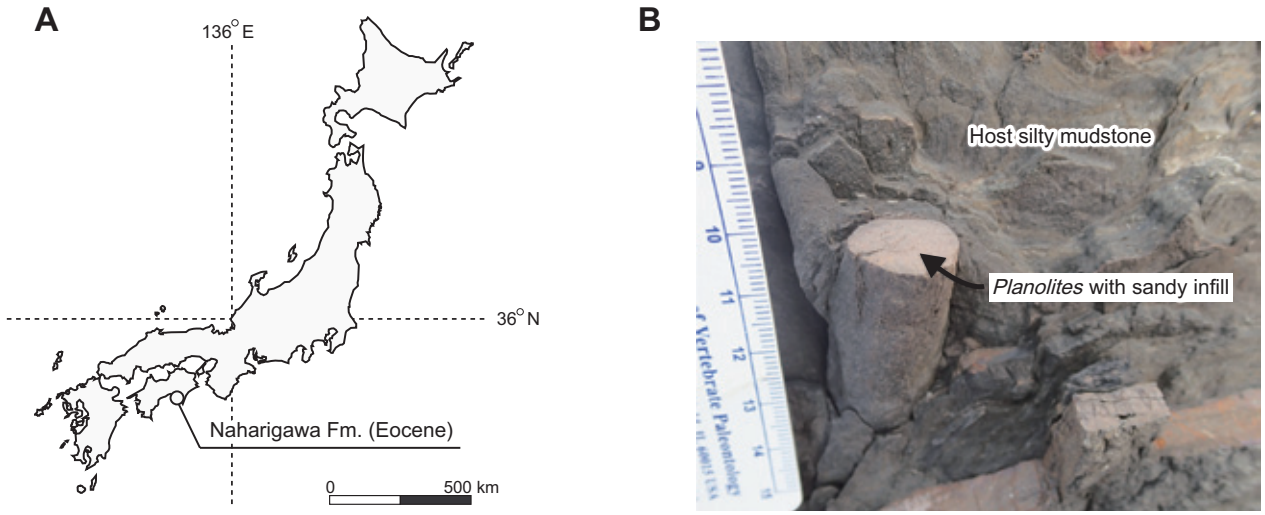

Fig. 2 (A) Locality map of the Eocene Naharigawa Formation. (B) Well preserved *Planolites* isp. from the Naharigawa Formation. Note that the straight tubular burrow morphology.

unbranched, unlined, tubular straight burrow (**Fig. 2B**). The fill consists generally of homogeneous light-gray colored sandy material, and differs from the surrounding host silty mudstone of dark-gray color. Therefore, *Planolites* is the ideal material for applying **Fig. 1C** method. For quantifying the mudstone compactional thinning, field and laboratory

analyses was combined. In particular, burrow sizes and aspect ratios of the *Planolites* specimens were measured during the fieldwork. For measuring the burrow aspect ratio values, we carefully selected *Planolites* specimens whose perpendicular cross sections can be observed. Then, to measure the degree of differential compaction between sandy infill of *Planolites* and surrounding host mudstone (**Fig. 1C**), thin-section analysis was carried out. In addition, to precisely estimate the degree of mudstone compactional thinning, we determined the initial (i.e. pre-compactional) burrow aspect ratio of *Planolites* by calculating a number of burrow aspect ratio values of modern *Planolites* specimens using published photographs.

For quantitatively determining calcium abundance of the mudstone from the Naharigawa Formation, a single mudstone sample was analyzed by X-ray fluorescence (XRF) technique. The mudstone sample was analyzed by using an energy dispersive X-ray spectrometry (JSX-1000S of JEOL, Tokyo, Japan). Elemental composition of the sample was determined by fundamental parameter method (FP method).

4. Results

4. 1 Compactional thinning of the Naharigawa mudstone

A total of 102 *Planolites* specimens were measured during our fieldwork. Burrow diameter (=burrow width) ranges from 2.85 to 22.4 mm of the average value of 9.25 (±4.10) mm. Burrow aspect ratio (i.e. burrow width/burrow height) ranges from 0.75 to 4.62 of the average value of 1.58 (±0.60) (**Fig. 3A**). Although quite rare, 9 specimens (8.82 %) showed their burrow aspect ratio values of less than 1 (**Fig. 3A**).

For modern *Planolites*, a total of 28 specimens occurred in modern core sediments collected from both shallow- and deep-marine environments, which was published by several papers (Wetzel, 2008, 2010；La Croix et al., 2015), were

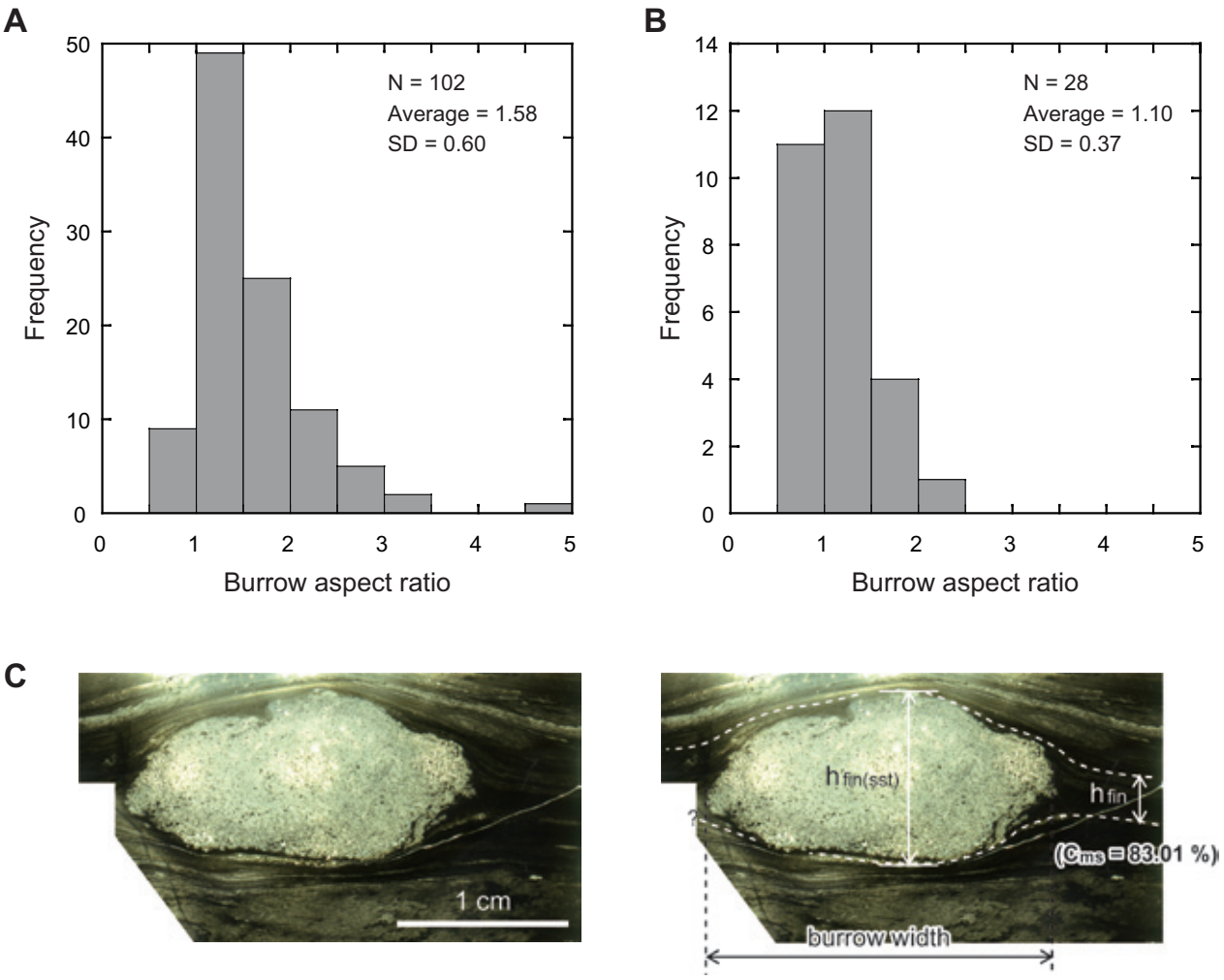

Fig. 3 Frequency distributions of burrow aspect ratio values of (A) *Planolites* from the Naharigawa Formation, and (B) *Planolites* from modern marine sediments. (C) Thin-section photomicrograph of the selected *Planolites* specimen from the Naharigawa Formation, with interpretations of several burrow parameters (i.e., $h_{fin\ (sst)}$, h_{fin}) and calculated C_{ms} value.

analyzed. As a result, burrow aspect ratio values range from 0.57 to 2.14 of the average value of 1.10 (± 0.37) (**Fig. 3B**). Among them, 11 specimens (39.29 %) showed their burrow aspect ratio values of less than 1 (**Fig. 3B**). The average value is significantly smaller ($p < 0.01$) than that of the fossil *Planolites* (= post compactional) specimens from the Naharigawa Formation, but is a bit (i.e. 10 %) larger than commonly hypothesized value (= 1). In this study, although many previous studies hypothesized that modern worm burrows have circular cross sections (i.e. initial burrow aspect ratio = 1 ; Lobza and Schieber, 1999), 1.10 is used as the initial, pre compactional burrow aspect ratio.

Based on observations of a number of thin sections, one *Planolites* specimen provides reliable data due to well-preserved deformation of silty laminae around *Planolites* (**Fig. 3C**). For this specimen, the burrow aspect ratio after compaction is 1.71, and the thickness between adjacent two deformed silty laminae (h_{fin}) is 26.42 % thinner than that of *Planolites* height ($h_{fin(sst)}$). Hence, considering the initial burrow aspect ratio is 1.10, C_{ms} for the Eocene Naharigawa Formation silty mudstone is calculated as 83.01 % (**Fig. 3C**).

4. 2 Geochemistry of the Naharigawa mudstone

Mudstone elemental composition determined by XRF analysis is summarized in **Table 1**, and the compositional value of each element is represented as weight percentage of its oxide. SiO_2 and Al_2O_3 exhibit the highest and second highest percentage of concentration, and CaO abundance in the Naharigawa mudstone sample is determined as 0.3647 wt. % (**Table 1**). In addition, CaO/Al_2O_3 and CaO/TiO_2 values are calculated as 0.02 and 0.49, respectively.

5. Discussion

The high C_{ms} value (83.01 %) for the mudstones from the Naharigawa Formation is supposed to be due to the low CaO abundance (0.3647 wt. %). As mentioned in section 1, the aim of this study is to propose the empirical relationship between the degrees of mudstone compaction and geochemical composition of mudstones. Therefore, for this purpose, we compiled available and unpublished data for both C_{ms} values and selected geochemical values (i.e. CaO, CaO/Al_2O_3, and CaO/TiO_2 values) for lithified mudstones of various ages. However, for compilation, we excluded C_{ms} data obtained from Neogene and Quaternary mudstones. This is because dry bulk density of clastic sedimentary rocks largely increases with increasing age from recent to early Miocene time, whereas dry bulk density of earlier rocks is nearly constant (Iwaya and Kano, 2005). This trend suggests that porosity reduction by compaction is still in progress for the Neogene and younger mudstones (Iwaya and Kano, 2005).

As a result, data from 11 examples (8 pre-Neogene mudstone data, 2 younger mudstone data, and 1 carbonate data) was compiled, which are summarized in **Table 2**. Using 8 pre-Neogene mudstone data, although data shows great variation, a significant negative correlation between the C_{ms} values and CaO abundances was recognized (**Fig. 4A**; $r = -0.75$; $p < 0.05$), suggesting that the degrees of mudstone compactional thinning are significantly affected by carbonate contents. This relationship quantitatively supports the idea from the previous experimental study (Kochman and Matyszkiewicz, 2013). Furthermore, based on the regression line, the degree of compactional thinning of limestone that consists mainly of fine-grained calcareous grains (i.e. micrite) may be estimated. CaO values in limestones generally show over 50 wt.% (e.g. Chutakositkanon et al., 2000), the degree of compactional thinning of micrite may considered to be ca. 30 % in general (**Fig. 4A**). Experimentally calculated degrees of compactional thinning of coarse-grained limestones range from 0 to 27.5 % (Kochman and Matyszkiewicz, 2013 ; **Fig. 4A**), which are

Table 1 Result of XRF analysis of the mudstone sample from the Naharigawa Formation.

	wt. %
Na_2O	1.2323
MgO	2.1645
Al_2O_3	17.9372
SiO_2	66.3546
P_2O_5	0.1705
SO_3	0.7004
K_2O	3.9665
CaO	0.3647
TiO_2	0.7386
V_2O_5	0.0150
Cr_2O_3	0.0098
MnO	0.0622
Fe_2O_3	6.1450
NiO	0.0030
ZnO	0.0129
Ga_2O_3	0.0032
As_2O_3	0.0017
Rb_2O	0.0200
SrO	0.0128
Y_2O_3	0.0029
ZrO_2	0.0241
CdO	0.0009
BaO	0.0570

lower than the value of standard micrite (ca. 30 %). This is reasonable because such coarse-grained limestones studied by Kochman and Matyszkiewicz (2013) are characterized by the development of reticulate or laminar rigid framework, resulting in small susceptibility to mechanical compaction.

In addition, the C_{ms} values are well correlated with the Ca concentrations normalized to terrigenous material (i.e. CaO/Al_2O_3, CaO/TiO_2 ; **Fig. 4B, C**), which are considered as proxies for relative contribution of non-terrigenous (i.e. biogenic) carbonates. Although these correlations are statistically not significant ($p>0.05$; **Fig. 4B, C**), these results may further support the idea that the degree of

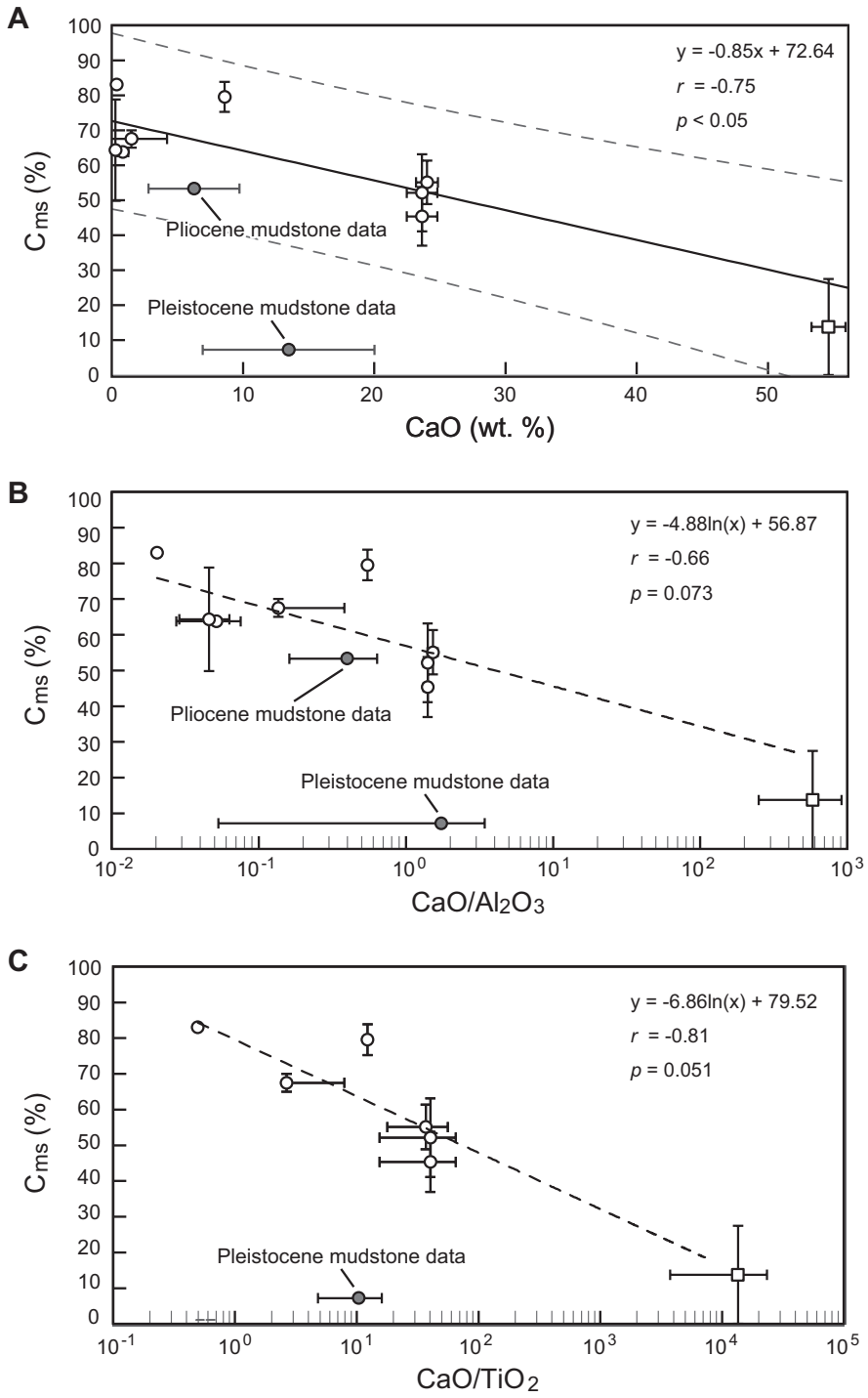

Fig. 4 Empirical relationships between the degrees of compactional thinning and (A) CaO values, (B) CaO/Al_2O_3 values, and (C) CaO/TiO_2 values. Gray dashed lines in Fig. 4A represent 95 % confidence interval. Gray circles represent data from Neogene and Quaternary mudstones, and open square represents data from limestone with rigid framework. Regression lines were calculated by using 8 pre-Neogene mudstone data (A, B) and 6 pre-Neogene mudstone data (C), respectively.

Table 2 Compiled dataset of C_{ms} values and geochemical compositions, which is used for calculating the empirical relationships illustrated in Fig. 4. Each value is represented as the average ± standard deviation, except for one data (see * in Table 2). Note that methods for geochemical analysis are different depending on each reference.

Material	Locality	Age	Calculated Cms (%)	CaO (wt.%)	CaO/Al_2O_3	CaO/TiO_2	Method		Reference, or data source	Note
							Cms calculation	Geochemical measurement		
Phosphorous coprolites	Osawa Formation, Japan	Early Triassic	79.54 ± 4.31 (n = 2)	8.59 (n = 1)	0.55 (n = 1)	12.27 (n = 1)	Fig. 1A	XRF	Nakajima and Izumi (2014)	
Carbonate concretions	Serra Alta Formation, Brazil	Permian	63.75 (n = 1)	0.84 ± 0.42 (n = 4)	0.051 ± 0.024 (n = 4)	No data	Fig. 1A	ICP-OES	Goldberg and Humayun (2010); Bondioli et al. (2015)	
Carbonate concretions	Bardo Unit, Sudetes Mountains, Poland	Early Carboniferous	64.32 ± 14.47 (n = 3)	0.28 ± 0.10 (n = 5)	0.046 ± 0.017 (n = 5)	No data	Fig. 1A	XRF	Bojanowski et al. (2014)	
Trace fossils (*Planolites*)	Kokumoto Formation, Japan	Pleistocene	7.21 (n = 1)	13.48 ± 6.55 (n = 2133)	1.74 ± 1.68 (n = 2133)	10.42 ± 5.61 (n = 2133)	Fig. 1B	XRF core scanner	Nishida et al. (2016); Izumi et al. (unpubl. data)	Unlithified silty sediments; data are excluded when calculating regression lines
Trace fossils (*Phymatoderma*)	Shiramazu Formation, Japan	Pliocene	53.32 (n = 1)	6.26 ± 3.46 (n = 32)	0.40 ± 0.24 (n = 32)	No data	Fig. 1B	SEM-EDS	Izumi (2013, 2015)	Data are excluded when calculating regression lines
Trace fossils (*Chondrites*)	Posidonia Shale, Germany	Early Jurassic	55.11 ± 6.23 (n = 23)	24.02 ± 0.83 (n = 11)	1.52 ± 0.12 (n = 11)	36.92 ± 19.14 (n = 11)	Fig. 1B	SEM-EDS	Izumi (2014b); Izumi et al. (2014)	
Trace fossils (*Chondrites*)	Punta La Llastra section, Spain	Early Jurassic	45.35 ± 8.38 (n = 15)	23.64 ± 1.16 (n = 7)	1.40 ± 0.09 (n = 7)	40.22 ± 24.85 (n = 7)	Fig. 1B	SEM-EDS	Izumi et al. (2014, unpubl. data)	
Trace fossils (*Phymatoderma*)	Punta La Llastra section, Spain	Early Jurassic	52.12 ± 11.02 (n = 6)	23.64 ± 1.16 (n = 7)	1.40 ± 0.09 (n = 8)	40.22 ± 24.85 (n = 8)	Fig. 1B	SEM-EDS	Izumi et al. (2014)	
Trace fossils (indeterminate burrows)	Chattanooga Shale, USA	Late Devonian	67.50 ± 2.50 (n = 2)	1.50 ± 2.72 (n = 10)	0.14 ± 0.24 (n = 10)	2.65 ± 5.25 (n = 10)	Fig. 1B	XRF	Lobza and Schieber (1999); Li and Schieber (2015)	
Trace fossils (*Planolites*)	Naharigawa Formation, Japan	Eocene	83.01 (n = 1)	0.36 (n = 1)	0.020 (n = 1)	0.49 (n = 1)	Fig. 1C	XRF	This study	
Bedded limestones	Kraków-Czestochowa Upland, Poland	Late Jurassic	0-27.5*	54.62 ± 1.30 (n = 27)	581.03 ± 331.50 (n = 27)	13547.82 ± 9803.03 (n = 27)	Experimental oedometric method	ICP-OES	Matyszkiewicz et al. (2012); Kochman and Matyszkiewicz (2013)	

* Open squres in Fig. 4 are plotted as 13.75 ± 13.75, because average and standard deviation data are not shown in the reference paper.

mudstone compactional thinning decreases with increasing carbonate content.

Despite the small number of compiled data, our study provides the first quantitative empirical relationships between the degrees of mudstone compaction and geochemical compositions.

Furthermore, it is worthwhile to emphasize that the obtained relationship between C_{ms} and CaO values (**Fig. 4A**) may hold only for completely lithified mudstones of Paleogene or older ages, because unlithified muddy sediments of younger age (e.g., Neogene, Quaternary) were generally less affected by mechanical compaction than older lithified mudstones (Iwaya and Kano, 2005). For example, the C_{ms} value of the unlithified Pleistocene silty sediments of the Kokumoto Formation, Kazusa Group, central Japan was calculated as 7.21 % (**Table 2**; **Fig. 4**), although CaO content of the Kokumoto Formation is 13.48 ± 6.55 wt. % (Izumi et al., unpublished data; **Table 2**). The data is therefore plotted significantly below the obtained correlation line (**Fig. 4A**; gray plot). According to the previous experimental study, porosity of the silty sediments from the Kokumoto Formation ranges from ca. 40 to 50 % (Inami, 1983). Silty sediments of ca. 40 to 50 % porosity are classified as viscous compaction stage as defined by Hoshino and Inami (1977). Physical property of such sediments is viscous liquid, rather than solid (Hoshino and Inami, 1977), suggesting that sediments are not fully consolidated.

In summary, except for the Neogene and younger sediments, the quantitative empirical relationship between the degrees of sediment physical compaction and geochemical compositions was proposed for the first time (**Fig. 4**). In many cases, directly calculating the C_{ms} values by using methods illustrated in **Fig. 1** is much more difficult than determining geochemical compositions by XRF measurements. Therefore, the proposed relationship (**Fig. 4**) is very helpful for quantitatively estimating the degree of sediment compactional thinning, as long as CaO contents (and Al_2O_3, TiO_2 values if any) in sediment samples are measured. However, because the number of data is quite limited, further research is required to establish more solid empirical relationships.

6. Conclusions

In this study, the empirical relationship between the degree of compactional thinning (C_{ms}) and geochemical composition for fully lithified mudstones was quantitatively estimated. To provide new data, fieldwork of the Eocene Naharigawa Formation, Kochi Prefecture, Japan, and lab analyses of the collected mudstone samples (e.g. thin-section analysis, geochemical analysis) were carried out. The obtained results were considered to propose the specific empirical relationship between the C_{ms} and geochemical composition, with compilation of previous available data. Based on the compilation, a significant and strong negative correlation between the degrees of sediment compactional thinning and CaO abundances was recognized ($r = -0.75$; $p < 0.05$). In addition, degrees of sediment compactional thinning are well correlated with Ca concentration normalized to terrigenous material (i.e. CaO/Al_2O_3, CaO/TiO_2). Our compilation results indicate that the degree of mechanical compaction of sediments is significantly affected by carbonate content. Although the obtained relationship may hold only for fully lithified mudstones, it is helpful for quantitatively estimating the degree of compactional thinning for any mudstone-dominated succession, as long as geochemical composition of the mudstone is determined. Assessing accurately the thickness changes of mudstones during compaction is important for estimating precise sedimentation rates, reconstructing and understanding cross stratification features, and interpreting specific sedimentary structures.

Acknowledgements

The authors would like to thank D.B. Kemp (University of Aberdeen) for his useful suggestions, discussion, and English editing. Thanks are also due to R. Yamamoto (Kokushikan University), T. Shibata (Agency for Cultural Affairs), K. Wada and T. Shirai (Muroto Geopark Promotion Committee) for their kind help during fieldwork, and M. Kikuchi (JEOL) for XRF measurements. A portion of this work was supported by research grant from the Japan Society for the Promotion of Science (grant no. 15J08821).

References

Bojanowski, M.J., Barczuk, A., Wetzel, A., 2014. Deep-burial alteration of early-diagenetic carbonate concretions formed in Palaeozoic deep-marine greywackes and mudstones (Bardo Unit, Sudetes Mountains, Poland). Sedimentology 61, 1211-1239.

Bondioli, J.G., Matos, S.A., Warren, L.V., Assine, M.L., Riccomini, C., Simões, M.G., 2015. The interplay between event and background sedimentation and the origin of fossil-rich carbonate concretions : a case study in Permian rocks of the Paraná Basin, Brazil. Lethaia 48, 522-539.

Chutakositkanon, V., Charusiri, P., Sashida, K., 2000. Lithostratigraphy of Permian marine sequences, Khao Pun Area, central Thailand : Paleoenvironments and tectonic history. Tha Island Arc 9, 173-187.

Devaney, K.A., Wilkinson, B.H., Van Der Voo, R., 1986. Deposition and compaction of carbonate clinothems : The

Silurian Pipe Creek Junior complex of east-central Indiana. Geological Society of America Bulletin 97, 1367-1381.

Gerard, J., Bromley, R.G., 2008. Ichnofabrics in Clastic Sediments. Applications to Sedimentological Core Studies. A Practical Guide. J. Gerard, Madrid, 100 p.

Goldberg, K., Humayun, M., 2010. The applicability of the Chemical Index of Alteration as a paleoclimatic indicator: An example from the Permian of the Paraná Basin, Brazil. Palaeogeography, Palaeoclimatology, Palaeoecology 293, 175-183.

Hoshino, K., Inami, K., 1977. Stages of compaction as defined from change of mechanical properties. Journal of the Japanese Association of Petroleum Technologists 42, 90-99.

Inami, K., 1983. On the compaction of mudstone from Kazusa Group in the Boso Peninsula, Chiba Prefecture, central Japan. Bulletin of the Geological Survey of Japan 34, 207-216.

Inami, K., Hoshino, K., 1974. Compressibility and compaction of clastic sedimentary rocks. Journal of the Japanese Association of Petroleum Technologists 39, 357-365 (in Japanese).

Iwaya, T., Kano, K., 2005. Rock densities for the geologic units in the Japanese Islands: an estimate from the database PROCK (Physical Properties of Rocks of Japan). Journal of the Geological Society of Japan 111, 434-437 (in Japanese).

Izumi, K., 2013. Geochemical composition of faecal pellets as an indicator of deposit-feeding strategies in the trace fossil *Phymatoderma*. Lethaia46, 496-507.

Izumi, K., 2014. Isotopic and mineralogical variations in the infill of *Chondrites* from organic-rich black shale (Posidonia Shale, Germany) for assessing the mode of colonization. Spanish Journal of Palaeontology 29, 107-116.

Izumi, K., 2015. Deposit feeding by the Pliocene deep-sea macrobenthos, synchronized with phytodetritus input: Micropaleontological and geochemical evidence recorded in the trace fossil *Phymatoderma*. Palaeogeography, Palaeoclimatology, Palaeoecology 431, 15-25.

Izumi, K., Rodríguez-Tovar, F.J., Piñuela, L., García-Ramos, J.C., 2014. Substrate-independent feeding mode of the ichnogenus *Phymatoderma* from the Lower Jurassic shelf-sea deposits of central and western Europe. Sedimentary Geology 312, 19-30.

Katto, J., Taira, A., 1978. Lithofacies and sedimentary environments of Muroto-Hanto Group. Chishitsu News 287, 21-31 (in Japanese, title translated).

Kochman, A., Matyszkiewicz, J., 2013. Experimental method for estimation of compaction in the Oxfordian bedded limestones of the southern Kraków-Częstochowa Upland, southern Poland. Acta Geologica Polonica 63, 681-696.

La Croix, A.D., Dashtgard, S.E., Gingras, M.K., Hauck, T.E., MacEachern, J.A., 2015. Bioturbation trends across the freshwater to brackish-water transition in rivers. Palaeogeography, Palaeoclimatology, Palaeoecology 440, 66-77.

Li, Y., Schieber, J., 2015. On the origin of a phosphate enriched interval in the Chattanooga Shale (Upper Devonian) of Tennessee-A combined sedimentologic, petrographic, and geochemical study. Sedimentary Geology 329, 40-61.

Lobza, V., Schieber, J., 1999. Biogenic sedimentary structures produced by worms in soupy, soft muds: Observations from the Chattanooga Shale (Upper Devonian) and experiments. Journal of Sedimentary Research 69, 1041-1049.

Matyszkiewicz, J., Kochman, A., Duś, A., 2012. Influence of local sedimentary conditions on development of microbialites in the Oxfordian carbonate buildups from the southern part of the Kraków-Częstochowa Upland (South Poland). Sedimentary Geology 263-264, 109-132.

Mondol, N.H., Bjørlykke, K., Jahren, J., Høeg, K., 2007. Experimental mechanical compaction of clay mineral aggregates-Changes in physical properties of mudstones during burial. Marine and Petroleum Geology 24, 289-311.

Nakajima, Y., Izumi, K., 2014. Coprolites from the upper Osawa Formation (upper Spathian), northeastern Japan: Evidence for predation in a marine ecosystem 5 Myr after the end-Permian mass extinction. Palaeogeography, Palaeoclimatology, Palaeoecology 414, 225-232.

Nara, M., Ikari, Y., 2011. "Deep-sea bivalvian highways": An ethological interpretation of branched *Protovirgularia* of the Paleogene Muroto-Hanto Group, southwestern Japan. Palaeogeography, Palaeoclimatology, Palaeoecology 305, 250-255.

Nara, M., Ikari, Y., 2015. Stop 4: Sedimentology and paleoecology of deep sea turbiditic systems of the Naharigawa Formation. In: Nara, M. (ed.), Field Trip Guidbook: Neo- and paleo-ichnological sites of Kochi Prefecture, SW Japan, pp. 28-31.

Nishida, N., Kazaoka, O., Izumi, K., Suganuma, Y., Okada, M., Yoshida, T., Ogitsu, I., Nakazato, H., Kameyama, S., Kagawa, A., Morisaki, M., Nirei, H., 2016. Sedimentary processes and depositional environments of a continuous marine succession across the Lower-Middle Pleistocene boundary: Kokumoto Formation, Kazusa Group, central Japan. Quaternary International 397, 3-15.

Potter, P.E., Maynard, J.B., Depetris, P.J., 2005. Mud and Mudstones: Introduction and Overview. Springer, Berlin, 304 p.

Schieber, V., 2003. Simple gifts and buried treasures - Implications of finding bioturbation and erosion surfaces in black shales. The Sedimentary Record 1, 4-8.

Taira, A., Tashiro, M., Okamura, M., Katto, J., 1980. The geology of the Shimanto Belt in Kochi Prefecture, Shikoku, Japan. In: Taira, A., Tashiro, M. (eds.), Geology and Paleontology of the Shimanto Belt: Selected Papers Honouring Professor J. Katto. Kochi, pp. 319-389 (in Japanese).

Taira, A., Katto, J., Tashiro, M., Okamura, M., Kodama, K., 1988. The Shimanto Belt in Shikoku, Japan-evolution of Cretaceous to Miocene accretionary prism. Modern Geology 12, 5-46.

Taira, A., Byrne, T., Ashi, J., 1992. Photographic Atlas of an Accretionary Prism: Geologic Structures of the Shimanto Belt, Japan. University of Tokyo Press, Tokyo, 124 p.

Velde, B., 1996. Compaction trends of clay-rich deep sea sediments. Marine Geology 133, 193-201.

Wetzel, A., 2008. Recent bioturbation in the deep South China Sea: A uniformitarian ichnologic approach. Palaios23, 601-615.

Wetzel, A., 2010. Deep-sea ichnology: Observations in modern sediments to interpret fossil counterparts. Acta Geologica Polonica 60, 125-138.